Synthesis and Characterization of $Cu_{2-x}S$ structures by Different Chemical Routes for Electronic Applications

João V. M. Lima[a] [ID], *Rafael A. Silva[a]* [ID], *Stevan B. O. Santos[a]* [ID], *Carlos F. O. Graeff[a,b]* [ID],

Luis V. A. Scalvi[a,b]* [ID]

[a]Universidade Estadual Paulista (Unesp), Faculdade de Ciências, Programa de Pós-Graduação em Ciência e Tecnologia de Materiais, 17033-360, Bauru, SP, Brasil.
[b]Universidade Estadual Paulista (Unesp), Faculdade de Ciências, Departamento de Física, 17033-360, Bauru, SP, Brasil.

Copper sulfides are materials with different technological applications due to different possibilities of phases, which result in different properties. Thus, obtaining particles with different stoichiometry of the materials is of great interest. Two simple chemical routes were used to obtain copper sulfides ($Cu_{2-x}S$) particles of different phases and stoichiometry. One of the obtained powders was used for thin film deposition through resistive evaporation and characterized. From scanning electron microscopy the particle size was found as around 500 nm. The second route leads to non-stoichiometric powder with characteristic CuS, Cu_9S_5 and Cu_2S planes detected in the XRD diffractograms. Thin films from this route were also obtained by resistive evaporation. The amorphous film obtained after evaporation was submitted to thermal annealing at 200 ° C/2h, becoming semi-crystalline. The deposited film showed good adhesion to the substrate and low roughness, in addition to a bandgap of 2.5 ± 0.1 eV and a resistivity of $1x10^{-2}$ Ω.cm, values in good agreement with those reported in the literature. The techniques used here proved to be of good quality for deposition of copper sulfide films, and can be used as a simpler alternative in addition to commonly used for deposition of copper sulfide films.

Keywords: *Copper Sulfide, Chemical Routes, Resistive Evaporation.*

1. Introduction

Copper sulfide ($Cu_{2-x}S$) has received considerable attention due to its potential applicability as coating for solar cells[1,2], radiation filters for windows, electroconductive coatings on organic polymers[3], cathode in lithium batteries[4], and as active layer in memory switching devices[5]. In addition, in the form of nanostructures, this compound may be applied in photocatalysis, solar cell, supercapacitors and biomedical applications[2]. The various application possibilities are due to the various existing $Cu_{2-x}S$ phases, which produce distinct optical, electronic and structural properties[6].

The different phases of copper sulfide range from the copper-rich chalcocite (Cu_2S) to villamaninite (CuS_2) with rather less copper, and other intermediate phases, such as djurleite ($Cu_{1.97}S$), digenite ($Cu_{1.8}S$), anilite ($Cu_{1.75}S$), geerite ($Cu_{1.6}S$), espionkopita ($Cu_{1.4}S$), yarrowite ($Cu_{1.2}S$) and covellite (CuS)[2]. All phases produce typically p-type semiconductors due to the existence of copper vacancies in thelattice[2]which act as acceptors in the matrix. Moreover, the optical bandgap varies from 0.6 to approximately 2.35 eV depending on stoichiometry[7], which leads to distinct absorptions edges that can vary from near-infrared to visible. Although for many years the nature of bandgap transition was under discussion, due to the appearance of absorption peaks in the UV-Vis and NIR spectrum, theoretical studies, based on the Moss-Burstein effect, rule out the possibility of an indirect transition for all phases[2].

Currently, different synthesis methods are being used for the deposition of $Cu_{2-x}S$ thin films, such as chemical vapor deposition (CVD)[6], sputtering[8]and chemical bath deposition. However, as pointed out by Grozdanov[9], films deposited by chemical bath on smooth substrates present problems of adhesion and low uniformity. Therefore, there is great interest in alternative techniques for deposition of $Cu_{2-x}S$ that are simpler when compared to CVD and sputtering, and that have good adhesion to the substrate and good structural characteristics.

Keeping that in mind, this work presents the description of two chemical routes and their parameters to obtain $Cu_{2-x}S$ particles with distinct stoichiometries, so that they can be used in the applications such as those described above. The obtained powders allow the deposition of thin films by a combined technique, which uses the powder obtained by chemical route and the film deposition by resistive evaporation, which represents an alternative to the use of routes purely chemical. Besides the improvements on adhesion of film to the substrate and the homogeneity, this combined technique allows innovation concerning deposition of sample distinct shapes, such as nanocomposites or heterostructures.

*e-mail: luis.scalvi@unesp.br

2. Experimental

The $Cu_{2-x}S$ powders were obtained from two different routes, the first of them was adapted from the work of I. Grozdanov[9], while the second one was adapted from the route used in works of Congiu et al. and Lima et al. [10]. The routes are presented separately below, in order to facilitate the discussion of the results.

Route 1: For a total solution of 100 ml, Copper Sulfate ($CuSO_4$) and sodium thiosulfate ($Na_2S_2O_3$) were mixed, both dissolved in deionized water. At this point, the initially blue solution turns green due to the reduction from Cu (II) to Cu (I) by the thiosulfate. Then, deionized water was used to increase the volume of the solution to 100 ml. The bath pH was maintained at 5, adjusting with acetic acid. The solution was then kept under stirring at fixed temperature until the end of the reaction. In these conditions, there is a change in the color of the solution until a brown precipitate starts to form on the beaker bottom. Then, the solution was transported to an Excelsa II 206 BL centrifuge, and the powder obtained was macerated and taken to a EDGCON 3P oven for heat treatment. The molar ratio between copper and sulfur, the temperature and agitation time of the bath, the final color of the solution and the temperature and time of thermal annealing of the powder depend on the desired stoichiometry and are described in Table 1.

Route 2: A solution with 1.5 M sodium thiosulfate ($Na_2S_2O_3$) and 0.5 M copper nitrate $Cu(NO_3)_2$ with pH 6 were used as precursors to obtain the $Cu_{2-x}S$ powder. This solution was subjected to a heating process, followed by filtration and washing with deionized water and isopropyl alcohol. Then, the powder obtained from the filtration is heated to 80 °C/ 3 h and is used for the deposition of $Cu_{2-x}S$ thin films. The samples prepared from this route are nominated S_4, to facilitate the discussion of the results.

Thin films of $Cu_{2-x}S$ were deposited from the S_1 powder sample in a Boc Edwards Auto 500 evaporator. The powder was placed inside a metallic crucible of tungsten (W), with a boat format. The resulting film thickness was 40 nm, which was measured with the help of a quartz sensor coupled to the evaporation system. The resistive evaporation technique for the deposition of $Cu_{2-x}S$ films was chosen due to be a relatively inexpensive alternative, compared to techniques such as CVD and sputtering. It is important to note that due to the rapid evaporation of sulfur, for large temperature variations, there is a loss of material due to the powder "jumping" from the crucible. Therefore, slow and gradual heating is necessary to avoid possible losses of material, and a highest pressure ("minimum vacuum") of ~$5x10^{-6}$ Torr is recommended to start the evaporation. In order to investigate the electrical transport in the material, metallic In contacts were evaporated on the surface of the film. The final architecture of the sample is shown in Figure 1.

X-ray diffraction measurements were performed with a Rigaku D/MAX-2100/PC diffractometer, using CuKα radiation (1.5405 Å), equipped with a Ni filter to attenuate the Kβ radiation, with a scanning rate of 1°/min, in the thin film configuration (2θ) with an incidence angle of 1.5°, and in the powder configuration (2θ/θ). With the aid of X-ray diffractograms the average crystallite size was estimated using the Scherrer equation[11].

In order to evaluate how the material behaves under temperature variation, thermogravimetry (TG) measurements

Table 1: Parameters used to obtain powders from Route 1.

Sample name	Powder stoichiometry	Molar ratio of precursors (Cu:S)	Temperature/Time bath	Color solution	Temperature/Time Themal Annealing
S_1	$Cu_{2-x}S$ (x = 0, 0.2 and 1)	1:2	70 °C/45 min	Brown	150 °C/1h
S_2	Cu_2S	1:2	45 °C/35 min	Brown	150 °C/10h
S_3	CuS	1:3	70 °C/45 min	Blue	Without thermal annealing
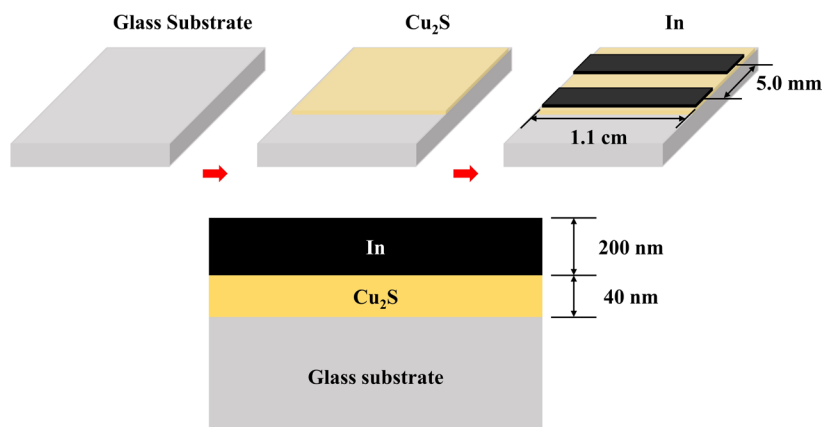
Figure 1. Sample architecture prepared from the resistive evaporation of S_1 powder. The dimensions of Cu_2S thin films and In contacts are shown in the image.

were performed in a NETZSCH STA 449 F3 equipment. The analysis was carried out in a dry air atmosphere (70 ml/min), in a temperature range of 28 to 820 °C, using a mass of 4.7 mg of the copper sulfide materials.

Scanning electron microscopy (SEM) measurements were performed in a microscope Zeiss EVO 15, equipped with an EDS sensor from Oxford Instruments. With that, it was possible to verify the particle size of the synthesized powders. Confocal microscopy measurements were performed in a Leica DCM 3D microscope, equipped with blue LED (emission centered at 460 nm), to study homogeneity and to obtain the mean square roughness (RMS) of the developed film surface.

Optical characterization was performed with transmittance spectroscopy, in a scanning range from 1800 to 200 nm (increasing energy) in a Perkin Elmer spectrometer, model Lambda 1050 Uv /Vis/Nir spectrometer. From the obtained spectrum, it was possible to estimate the optical bandgap of the material, through the Tauc plot[12].

Current vs voltage (IxV) measurements were performed at room atmosphere and ambient temperature on the PaiosFLUXiM equipment, while measurements at low pressure (about 10^{-5} torr) and with a temperature decrease of up to 30 K were performed on a He-closed cycle cryostat (from Janis) coupled to a Keithley electrometer. In the final sample design for electrical measurements, as shown in Figure 1, Cu$_2$S film are 40 nm thick and metallic In layer is about 200 nm thick, both thickness evaluated by a quartz piezoelectric sensor. The distance between contacts is 0.5 cm and the contact width is about 1.01 cm. IxV measurements were carried out at distinct temperatures (30, 50, 100, 150, 200, 250 and 300 K), and the resistivity at each temperature was obtained by linear regression of the IxV curve in conjunction with sample conductive channel dimensions.

3. Results and Discussion

Figure 2 shows XRD diffractograms for powders samples S$_1$ to S$_4$. Diffractograms for samples S$_1$ to S$_3$, obtained from route 1, are in Figure 2a. The powder obtained following the parameters of sample S$_1$ is non-stoichiometric, where it was possible to observe the presence of three phases of Cu$_{2-x}$S. Miller indices in red color refer to Cu$_2$S planes

with cubic crystalline structure (JCPDS 053-0522), while Miller indices in black refer to Cu$_9$S$_5$ with rhombohedral crystalline structure of the Digenite phase (ICDD # 047-1748) and the indices identified in blue are related to the CuS stoichiometry of hexagonal crystalline structure in the Covelite phase (ICDD # 006-0464). Using the same powder as a precursor and changing the thermal annealing, as can be seen in Table 1 (sample S$_2$), the only peaks identified refer to cubic Cu$_2$S (red). This is due to the elimination of sulfur from the precursor powder, since it has lower boiling point than copper, making the copper-to-sulfur ratio in the material 2 to 1.

When the molar ratio Cu and S changes to 1:3, as can be seen in Table 1 for sample S$_3$, the peaks obtained in the X-ray diffractogram refer to the hexagonal CuS, Covelite phase (blue Miller indices). In this case, the decrease of the Cu: S ratio (increase in the S proportion) in the obtained powder is an expected result, since a greater molarity of the sulfur precursor is inserted during the synthesis of the material. The average crystallite size was calculated for these samples, using the Scherrer equation, assuming a spherical shape of the crystallites, in good agreement with the literature[11]. The average size of the crystallites for the samples from S$_1$ to S$_3$ are, respectively, 17.8, 21.1 and 6.1 nm, which means a considerable decrease in the size of the crystallite is observed when the proportion of sulfur is increased.

The X-ray diffractogram measured for the powder obtained through route 2 is shown in Figure 2b. As can be seen, the diffractogram indicates a non-stoichiometric Cu$_{2-x}$S powder and the appearance of several peaks makes it difficult to identify the Miller index associated with them, as well as to calculate the average size of the crystallites. However, as it is possible to verify through the works of Lima et al. [10] and Congiu et al. [7], this powder can be used for deposition of copper sulfide thin films by resistive evaporation. In the referred works, amorphous films are obtained right after the evaporation process, starting to present Cu$_{1,8}$S stoichiometry of Digenite phase (JCPDS # 23-0962) after thermal annealing of 200 °C/30 min.

Figure 3 shows TG analysis for all the samples, S$_1$ to S$_4$. The most relevant result for the issue treated in this paper is the mass gain that appears for all materials in the range of 266 to 296°C, depending on the phase of the material.
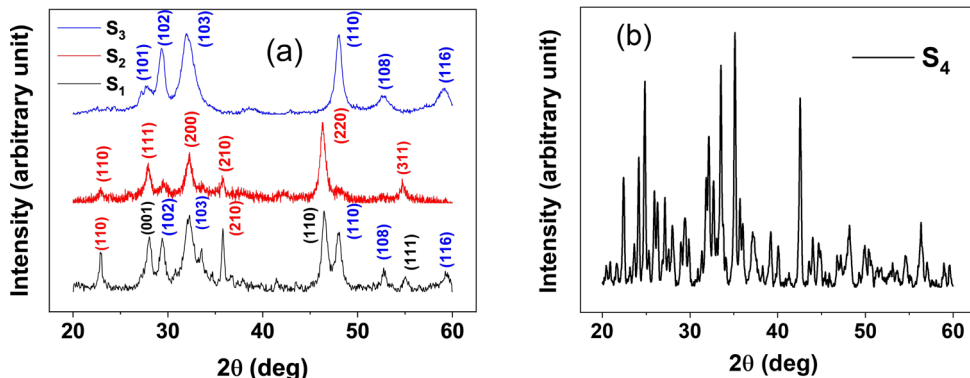
Figure 2. X-ray diffractagram for Cu$_{2-x}$S particles obtained from **(a)** route 1 and **(b)** route 2. Miller indices in red color refer to cubic Cu$_2$S (JCPDS 053-0522), in black refer to Cu$_9$S$_5$ with rhombohedral structure of Digenite phase (ICDD # 047-1748) and in blue are related to the hexagonal CuS in the Covelite phase (ICDD # 006-0464).
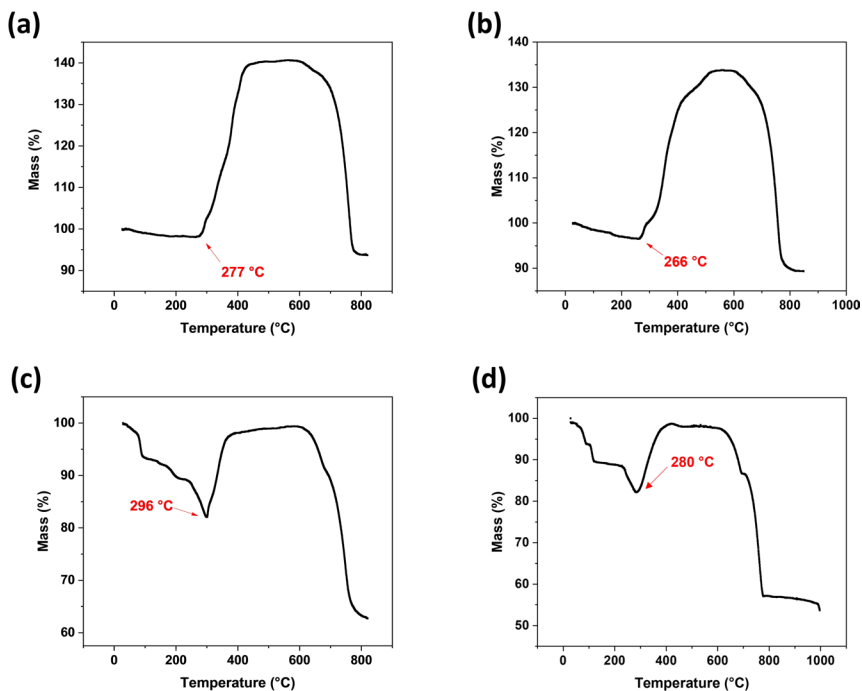
Figure 3. TG curves for samples **(a)** S_1, **(b)** S_2, **(c)** S_3 and **(d)** S_4.

This mass gain had already been reported in the works by Congiu et al. [7] and Lima et al. [10], being associated with copper oxidation. This is an important result as it justifies the choice of relatively low temperatures for the thermal annealing of $Cu_{2-x}S$ powders and films, which are 150 °C for powders and 200 °C for films. This implies that thermal annealing at higher temperatures, in order to eliminate a greater number of impurities and aiming at more crystalline films with less morphologic defects, must be carried out in inert atmospheres, poor in oxygen, so that the oxidation of copper is avoided.

From the results displayed in Figure 3 it is also possible to see that S_1 and S_2, which have copper-rich phases (Cu_2S), are those with the greatest increase in mass, exceeding the initial mass value by 40%. In this phase, the bonds between copper atoms, that have less binding energy, are broken by the increase in temperature and rebuilt with oxygen, leading to the observed increase in mass.

The behavior of sample S_4 is the closest to the behavior of sample S_3, which indicates that, despite being a non-stoichiometric powder, the CuS phase is supposedly more present in the sample. Considering that these samples have a higher sulfur proportion when compared to Cu_2S, it is possible to notice a more pronounced loss of mass at temperatures below 300 °C, which may be related to the elimination of sulfur from the material. As the atomic mass of sulfur (32.065 g/mol) is almost half of the atomic mass of copper (63.546 g/mol), the percentage of the mass of material lost due to the elimination of sulfur is more significant when the proportion of sulfur is higher, that is, when the Cu:S ratio is 1: 1.

Figure 4 shows SEM images for samples S_1 to S_4. From these images it is possible to observe the formation of particles with dimensions of approximately 500 nm.

Note that the particles are only dispersed in sample S_1, whereas they shown up agglomerated for the other samples. These agglomerates are not a problem for deposition of thin films in this work, since they will be evaporated, however, they must be dispersed depending on the desired application for this material, since agglomerated particles can hinder the dissolution of this material, or even result in non-homogeneous surfaces. One of the ways to get these particles to be more dispersed is by taking them to an aqueous medium, such as deionized water, and dispersing them with the aid of ultrasound vibration. Another alternative is to add a surfactant to the particulates, such as Triton X-100, because the separation from hydrophilic and hydrophobic chains in the surfactant[13], prevent the formation of micelles in particles of some materials, such as niobium pentoxide (Nb_2O_5)[14], and can also be used as a dispersant for clusters of the material treated here.

Figure 5a shows the X-ray diffractograms of films deposited by resistive evaporation technique after thermal annealing of 200 °C/1h, using the sample powder S_1 as precursor. The material presented a hexagonal crystalline structure of calcocyte phase in Cu_2S stoichiometry (JCPDS # 01-089-2670). The thickness of the deposited film was 40 nm and the average crystallite size, obtained from Scherrer's equation using the peak referring to the plane (002) is 13 nm. The work of Shinde et al. [11] shows that the crystallite size in Cu_2S films increases with increasing thickness of the deposited film, that is, a 130 nm thick Cu_2S film had an average crystallite size of 30 nm in the referred paper, becoming 250 nm for a 400 nm thick film. Thus, the result presented here, that the crystallite size is 13 nm for a 40 nm thick film is within the expected range. Figure SF1 in the supplementary information file presents the diffractogram for a resistively evaporated film from the non-stoichiometric powder (diffractogram
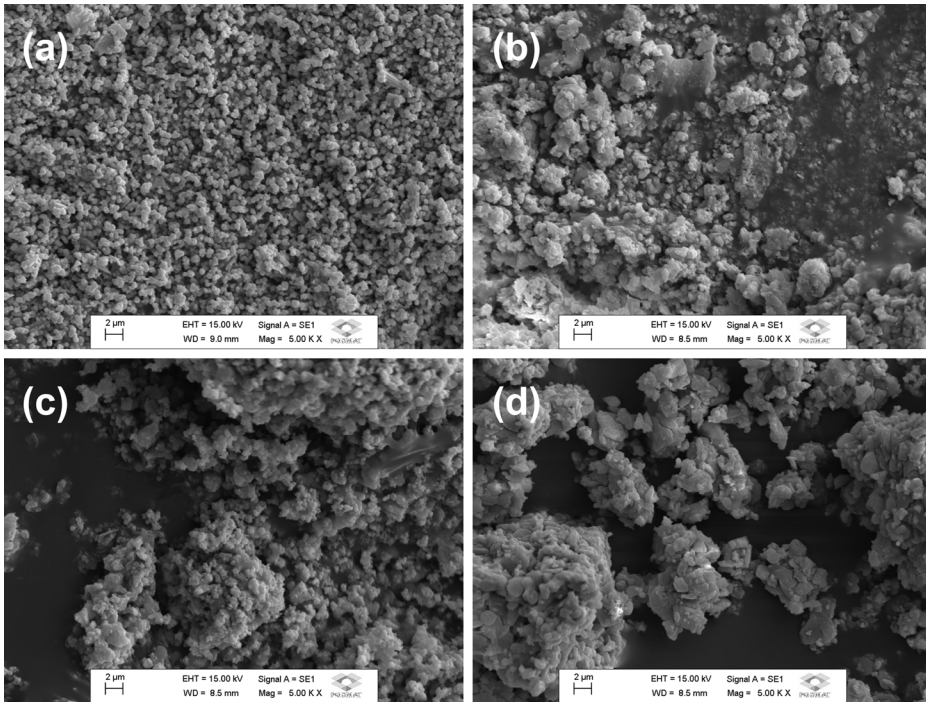
Figure 4. SEM images for Cu$_{2-x}$S powder samples. **(a)** S$_1$, **(b)** S$_2$, **(c)** S$_3$ and **(d)** S$_4$.
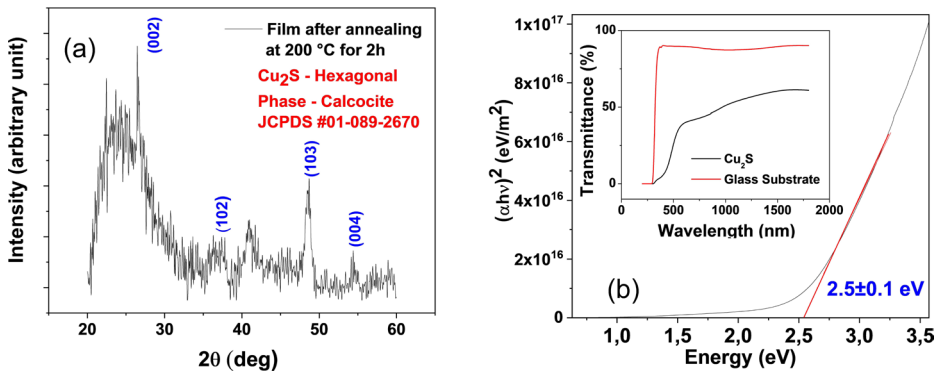
Figure 5. (a) X-ray diffractogram for the Cu$_2$S film and **(b)** bandgap evaluation for the Cu$_2$S film.

at Figure 2b), which, after thermal annealing at 200 °C for 30 min, shows peaks referring to hexagonal Cu$_{1.8}$S, of digenite phase (JCPDS 23-0962).

Figure 5b shows the estimate of the optical bandgap of the material using the Tauc plot method and, in detail, the transmittance spectrum of the deposited film and of the soda-lime glass substrate. For the Cu$_2$S film, a transmittance of approximately 60% is noted for a wavelength of 1800 nm. This transmittance drops smoothly, until it reaches about 40% at 600 nm. This behavior is similar (but less intense) to that obtained by Rastogi and Salkalachen[15] for Cu$_2$S samples with copper agglomerates on the film surface. In this way, we can induce the presence of copper in the samples presented in this work, however, in a smaller amount when compared to the referred work. Regardless of that, the fundamental absorption edge, which occurs around 500 nm, is in good agreement with the results found in the literature for Cu$_2$S films[16].

Couve et al.[17] reports that the transmittance of Cu$_2$S films decreases with increasing thickness, besides leading to a decrease in its optical bandgap. Therefore, the thickness of the film, along with its transmittance profile and bandgap, must be controlled according to the desired application.

The estimated value for its optical bandgap energy was E$_G$ = 2.5 ± 0.1 eV, in good agreement with the work of Grozdanov and Najdoski[16], where Cu$_2$S films presented a 2.4 eV bandgap (value also obtained through the Tauc plot). The values of E$_G$ found in the literature for copper sulfide are quite varied, as well as being extremely dependent on the form of material deposition (bulk, film or nanoparticles) [2]. However, studies agree that, when considering copper sulfide in the form Cu$_{2-x}$S (0≤x≤1), the E$_G$ value increases with the decrease of copper, with lower values being Cu$_2$S stoichiometry[2,16]. This is due to the Moss-Burstein effect, since, when the Cu:S ratio decreases, the formation of holes
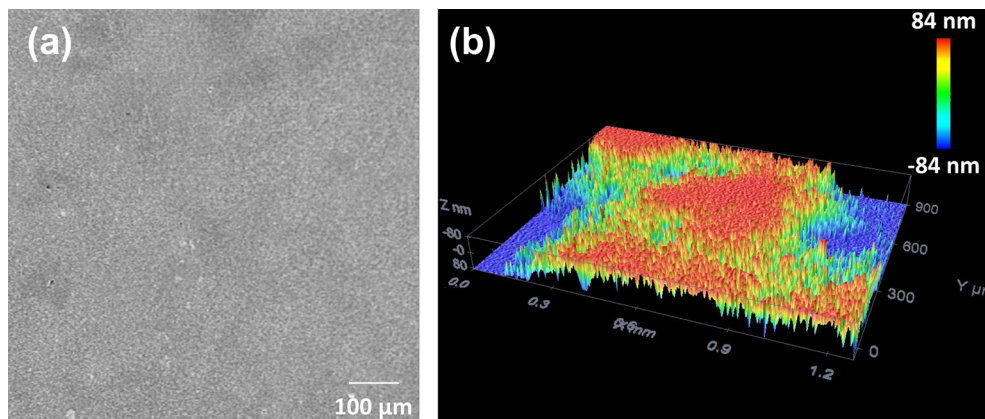
Figure 6. Confocal microscopy for Cu_2S film obtained from resistive evaporation. **(a)** surface mode and **(b)** topography mode.
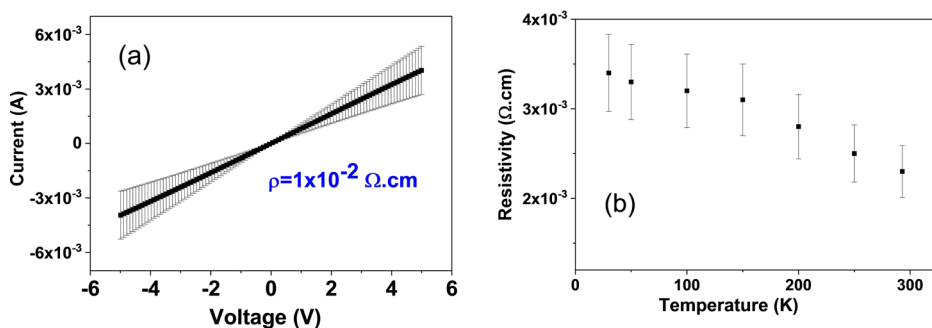
Figure 7. (a) Current vs. voltage for the Cu_2S film at 300K and **(b)** resistivity vs. temperature for the Cu_2S film.

close to the valence band top leads to the energy change of the lowest occupied energy level, changing the material's bandgap values. The supplementary information file presents evaluation of the optical bandgap of film with hexagonal $Cu_{1.8}S$, of digenite phase, obtained from the non-stoichiometric powder (S4) in Figure SF2.

Images obtained by confocal microscopy (Figure 6) with 10x magnification, show that the Cu_2S film has a rather homogeneous surface, and moreover, present a good adhesion to the soda-lime glass substrate. All the regions of the film present a similar surface of that shown here (Figure 6a). Edge deformation (blue regions in Figure 6b) are present in most of the images obtained in topography mode of confocal microscopy and has not been considered. The uniformity in the films grown in this work can be a result of the used deposition technique (resistive evaporation), a physical method in vacuum conditions ($5x10^{-6}$ torr). Grozdanov[9] points out problems of adhesion and uniformity of the film of Cu_2S deposited by chemical routes. Using a technique widely used in the literature for deposition of thin copper sulfide films on glass, it requires chemical attacks on the substrate surface or even deposition of other films prior to CuS, such as tin dioxide (SnO_2), to improve uniformity and adhesion. It is worth mentioning that the resistive evaporation for deposition of $Cu_{2-x}S$ thin films is a rather simple technique when compared to techniques such as CVD and Sputtering,

The IxV characteristic curve for Cu_2S with In contact, in range from -5 to 5 V, are shown in Figure 7a. Data are collected under room atmosphere and temperature. To make

connection between measurement devices and metallic In contact, a dot of silver paint were dropped below the point probe. The curve in Figure 7a represents the average of the results obtained in three devices, while the error bars represent the standard deviation of these results. Note that the curve obtained for the device showed an ohmic behavior. Considering the work function of In as 4.09 eV and the electronic affinity of copper sulfide as 4.1 eV [18], the height of the possible Schottky barrier formed between the semiconductor and the metallic contact of In is 2.5 eV[19]. Under ideal conditions for this ohmic behavior to exist, a high temperature would be necessary for thermionic conduction or tunneling conduction. However, it may can happen with the diffusion of In to Cu_2S. The formation of a thin highly doped layer just below the interface has been classically reported as explanation for ohmic behavior for other semiconductors[20], even for p-type ones[21]. Then, it might be the case here. The resistivity found for the material was $1x10^{-2}\Omega.cm$, in good agreement for Cu_2S films with similar characteristics found in the literature[22]. The supplementary information file presents resistivity of film with $Cu_{1.8}S$ stoichiometry in Figure SF3, also in good agreement with these data.

Figure 7b shows the resistivity x temperature curve for the Cu_2S sample, where it is possible to observe the semiconductor behavior of the samples, that is, a decrease in resistivity when the temperature is increased, due to the thermal excitation of carriers. In addition, it can be seen that the resistivity of the sample in vacuum at room temperature is approximately an order of magnitude lower when compared

to the sample at room atmosphere. A possible explanation is that reducing gases are adsorbed on the surface of the film, since has been reported[23,24] a decrease in the conductivity of p-type semiconductors in the presence of this sort of gases. Once the vacuum is done and the gases are desorbed, their conductivity increases. However, a more in-depth study about gases present in the atmosphere that adsorb on the surface of $Cu_{2-x}S$ needs to be done so that the hypothesis can be corroborated, since a few works are found in the literature concerning copper sulfides use for gas sensing, mostly pointing to its use for sensors of ammonia gas[25,26].

4. Conclusions

$Cu_{2-x}S$ particles were obtained through two rather simple chemical routes. The first route uses Copper Sulfate as a precursor to Cu, while the second uses Copper Nitrate. As a precursor to sulfur, sodium thiosulfate is used in both routes. Parameters of temperature and molar ratio between copper and sulfur precursors were studied in order to obtain different stoichiometries of the resulting material, aiming at different application possibilities. Through the X-ray diffractograms, it was possible to verify the formation of several stoichiometries, including CuS and Cu_2S powders, in addition to two non-stoichiometric powders. The powder particles are approximately 500 nm in diameter, as verified from SEM images.

Obtained powder from a chemical route gives birth to thin films of Cu_2S, which were deposited on glass substrate by resistive evaporation. Despite difficulties during evaporation, such as loss of stoichiometry of the evaporated material due to the rapid evaporation of sulfur, the films deposited by this combined technique showed good adhesion to the substrate and, characteristic not achieved through depositions by routes purely chemical. In addition, when compared to other techniques used for deposition of copper sulfide films, such as CVD and sputtering, resistive evaporation is a rather simpler technique that has shown to be of good quality in relation to structural, optical and electrical properties. The optical bandgap (2.5 eV) and the resistivity ($1x10^{-2}$ Ω.cm) of the Cu_2S film were evaluated and are in good agreement with works reported in the literature.

The $Cu_{2-x}S$ powder obtained in distinct stoichiometries by this combined technique is an alternative way of producing different sample geometries such as thin films, nanocomposites or heterostructures, which can be used in optoelectronic devices.

5. Acknowledgements

6. References

1. Selopal GS, Chahine R, Mohammadnezhad M, Navarro-Pardo F, Benetti D, Zhao H, et al. Highly efficient and stable spray assisted nanostructured Cu_2S/Carbon paper counter electrode for quantum dots sensitized solar cells. J Power Sources. 2019;436(308):226849. http://dx.doi.org/10.1016/j.jpowsour.2019.226849.

2. Roy P, Srivastava SK. Nanostructured copper sulfides: synthesis, properties and applications. CrystEngComm. 2015;17(41):7801-15. http://dx.doi.org/10.1039/C5CE01304F.

3. Naşcu C, Pop I, Ionescu V, Indrea E, Bratu I. Spray pyrolysis deposition of CuS thin films. Mater Lett. 1997;32(2-3):73-7. http://dx.doi.org/10.1016/S0167-577X(97)00015-3.

4. Chung J-S, Sohn H-J. Electrochemical behaviors of CuS as a cathode material for lithium secondary batteries. J Power Sources. 2002;108(1-2):226-31. http://dx.doi.org/10.1016/S0378-7753(02)00024-1.

5. Congiu M, Albano LGS, Nunes-Neto O, Graeff CFO. Printable ReRAM devices based on the non-stoichiometric junction $CuS/Cu_{2-x}S$. Electron Lett. 2016;52(22):1871-3. http://dx.doi.org/10.1049/el.2016.2901.

6. Kim KK, Hsu A, Jia X, Kim SM, Shi Y, Hofmann M, et al. Synthesis of monolayer hexagonal boron nitride on Cu foil using chemical vapor deposition. Nano Lett. 2012;12(1):161-6. http://dx.doi.org/10.1021/nl203249a.

7. Congiu M, Nunes-Neto O, De Marco ML, Dini D, Graeff CFO. $Cu_{2-x}S$ films as counter-electrodes for dye solar cells with ferrocene-based liquid electrolytes. Thin Solid Films. 2016;612(June):22-8. http://dx.doi.org/10.1016/j.tsf.2016.05.033.

8. Ghribi F, Alyamani A, Ben Ayadi Z, Djessas K, El Mir L. Study of CuS thin films for solar cell applications sputtered from nanoparticles synthesised by hydrothermal route. Energy Procedia. 2015;84(216):197-203. http://dx.doi.org/10.1016/j.egypro.2015.12.314.

9. Grozdanov I. A simple and low-cost technique for electroless deposition of chalcogenide thin films. Semicond Sci Technol. 1994;9(6):1234-41. http://dx.doi.org/10.1088/0268-1242/9/6/013.

10. Lima JVM, Boratto MH, Santos SBO, Scalvi LVA. Thermal Annealing Influence on the Properties of Heterostructure Based on 2at.%Eu Doped SnO_2 and $Cu_{1.8}S$. J Electron Mater. 2018;47(12):7463-71. http://dx.doi.org/10.1007/s11664-018-6687-6.

11. Shinde MS, Ahirrao PB, Patil JI, Patil RS. Thickness dependent electrical and optical properties of nanocrystalline copper sulfide thin films grown by simple chemical route. Indian J Pure Appl Phy. 2012;50:657-60.

12. Viezbicke BD, Patel S, Davis BE, Birnie DP 3rd. Evaluation of the Tauc method for optical absorption edge determination: ZnO thin films as a model system. Phys Status Solidi Basic Res. 2015;252(8):1700-10. http://dx.doi.org/10.1002/pssb.201552007.

13. Yang YJ, Corti DS, Franses EI. Effect of Triton X-100 on the stability of titania nanoparticles against agglomeration and sedimentation: A masked depletion interaction. Colloids Surf A Physicochem Eng Asp. 2017;516:296-304. http://dx.doi.org/10.1016/j.colsurfa.2016.12.026.

14. Lim E, Jo C, Kim H, Kim M-H, Mun Y, Chun J, et al. Facile synthesis of Nb_2O_5 @Carbon core-shell nanocrystals with controlled crystalline structure for high-power anodes in hybrid supercapacitors. ACS Nano. 2015;9(7):7497-505. http://dx.doi.org/10.1021/acsnano.5b02601.

15. Rastogi AC, Salkalachen S. Optical absorption behaviour of evaporated CuxS thin films. Thin Solid Films. 1982;97(2):191-9. http://dx.doi.org/10.1016/0040-6090(82)90228-0.

16. Grozdanov I, Najdoski M. Optical and electrical properties of copper sulfide films of variable composition. J Solid State Chem. 1995;114(2):469-75. http://dx.doi.org/10.1006/jssc.1995.1070.

17. Couve S, Gouskov L, Szepessy L, Vedel J, Castel E. Resistivity and optical transmission of Cu_xS layers as a function of composition. Thin Solid Films. 1973;15(2):223-31. http://dx.doi.org/10.1016/0040-6090(73)90046-1.

18. Goswami SK, Kim J, Hong K, Oh E, Yang Y, Yu D. Photocurrent and photovoltaic characteristics of copper sulfide nanowires grown by a hydrothermal method. Mater Lett. Elsevier. 2014;133:132-4. http://dx.doi.org/10.1016/j.matlet.2014.06.173.

19. Kasap SO. Principles of electronic materials and devices. 3rd ed. India: Tata McGraw-Hill; 2006.

20. Scalvi LVA, Degani MH. Substitutional donor related states and Au/Ge/Ni contacts to $Al_xGa_{1-x}As$. Philos Mag B Phys Condens Matter Struct Electron Opt Magn Prop. 1993;68(5):727-35. http://dx.doi.org/10.1080/13642819308220155.

21. Reemtsma J-H, Heime K, Schlapp W, Weimann G. p-type ohmic contacts to AlGaAs/GaAs heterostructures. Superlattices Microstruct. 1988;4(2):197-9. http://dx.doi.org/10.1016/0749-6036(88)90035-3.

22. Pathan HM, Desai JD, Lokhande CD. Modified chemical deposition and physico-chemical properties of copper sulfide (Cu_2S) thin films. Appl Surf Sci. 2002;202(1-2):47-56. http://dx.doi.org/10.1016/S0169-4332(02)00843-7.

23. Bejaoui A, Guerin J, Aguir K. Modeling of a p-type resistive gas sensor in the presence of a reducing gas. Sens Actuators B Chem. 2013;181:340-7. http://dx.doi.org/10.1016/j.snb.2013.01.018.

24. Mokoena TP, Swart HC, Motaung DE. A review on recent progress of p-type nickel oxide-based gas sensors: future perspectives. J Alloys Compd. 2019;805:267-94. http://dx.doi.org/10.1016/j.jallcom.2019.06.329.

25. Sagade AA, Sharma R. Copper sulfide (Cu_xS) as an ammonia gas sensor working at room temperature. Sens Actuators B Chem. 2008;133(1):135-43. http://dx.doi.org/10.1016/j.snb.2008.02.015.

26. Sagade AA, Sharma R, Sulaniya I. Enhancement in sensitivity of copper sulfide thin film ammonia gas sensor: effect of swift heavy ion irradiation. J Appl Phys. 2009;105(4):043701. http://dx.doi.org/10.1063/1.3053350.

Supplementary material

The following online material is available for this article:

Figure SF1 - X-ray diffractogram for film deposited by resistive evaporation, using the non-stoichiometric powder obtained from route 2.

Figure SF2 - Transmittance spectra for film deposited by resistive evaporation, using the non-stoichiometric powder obtained from route 2.

Figure SF3 - IxV curve obtained for film deposited by resistive evaporation, using the non-stoichiometric powder obtained from route 2.

Figure SF4 - Bode plot obtained for Cu_2S film.